Anal. Chem. **2010,** *82,* 1905–1910

Label-Free Biomarker Sensing in Undiluted Serum with Suspended Microchannel Resonators

Marcio G. von Muhlen,[†] Norman D. Brault,[‡] Scott M. Knudsen,[†] Shaoyi Jiang,[‡] and Scott R. Manalis*,[†]

Department of Biological Engineering and Mechanical Engineering, Massachusetts Institute of Technology, Cambridge, Massachusetts 02139, and Department of Chemical Engineering, University of Washington, Seattle, Washington 98195

Improved methods are needed for routine, inexpensive monitoring of biomarkers that could facilitate earlier detection and characterization of cancer. Suspended microchannel resonators (SMRs) are highly sensitive, batch-fabricated microcantilevers with embedded microchannels that can directly quantify adsorbed mass via changes in resonant frequency. As in other label-free detection methods, biomolecular measurements in complex media such as serum are challenging due to high background signals from nonspecific binding. In this report, we demonstrate that carboxybetaine-derived polymers developed to adsorb directly onto SMR SiO_2 surfaces act as ultralow fouling and functionalizable surface coatings. Coupled with a reference microcantilever, this approach enables detection of activated leukocyte cell adhesion molecule (ALCAM), a model cancer biomarker, in undiluted serum with a limit of detection of 10 ng/mL.

Improved methods for quantifying biomarkers in blood are necessary for earlier detection and characterization of cancer, with the ultimate goal of improving treatment.[1] Traditional detection methods are based on a sandwich configuration in which primary antibodies adsorbed on a surface concentrate a target molecule, a labeled secondary antibody provides specificity, and signal amplification is performed to detect physiologically relevant target concentrations. The classic example, enzyme-linked immunosorbent assay (ELISA), is widely used in clinical laboratories. Recent efforts have been directed toward making labeling approaches more sensitive and specific, less reagent-intensive, and easier to perform and multiplex. These include immuno-PCR,[2] rolling circle amplification,[3] proximity ligation,[4] protein chips,[5] microfluidic arrays,[6] Luminex,[7] and biobarcode nanoparticles.[8]

Label-free approaches are based on direct readout of target presence[9] and offer a simple one-step assay that conserves reagents and minimizes fluidic handling. Label-free surface plasmon resonance (SPR)[10] and quartz crystal microbalances[11] are routinely used for measuring biomolecular binding kinetics, but they are not widely applied to biomolecular detection because they tend to be less sensitive than labeled approaches and are prone to high background noise by nonspecific binding (fouling) from complex mixtures such as serum.[12] Mass spectroscopy can also be used for biomarker detection,[13] but high equipment costs limit the potential for routine widespread use.

The ideal label-free sensor would have high sensitivity (comparable to or better than ELISA, 0.1 ng/mL ALCAM limit of detection in a commercial kit[14]), require little or no sample preparation, enable multiplexed measurements, and be inexpensive to manufacture and use. Several approaches have been recently reported that push the boundaries of each of these characteristics. Armani et al. demonstrated optical microcavities with a 5 aM limit of detection of interleukin-2 in 10% serum.[15] Zheng et al. reported multiplexed detection with silicon nanowires, including prostate-specific antigen (PSA) at 0.9 pg/mL in desalted donkey serum.[16] SPR imaging mode for array-based simultaneous detection of hundreds of targets has been reported,[17,18] and array-

* To whom correspondence should be addressed. E-mail: scottm@media.mit.edu.

[†] Massachusetts Institute of Technology.

[‡] University of Washington.

(1) Hanash, S. M.; Pitteri, S. J.; Faca, V. M. *Nature* **2008**, *452*, 571–579.
(2) Sano, T.; Smith, C.; Cantor, C. *Science* **1992**, *258*, 120–122.
(3) Schweitzer, B.; Roberts, S.; Grimwade, B.; Shao, W.; Wang, M.; Fu, Q.; Shu, Q.; Laroche, I.; Zhou, Z.; Tchernev, V. T.; Christiansen, J.; Velleca, M.; Kingsmore, S. F. *Nat. Biotechnol.* **2002**, *20*, 359–365.
(4) Fredriksson, S.; Gullberg, M.; Jarvius, J.; Olsson, C.; Pietras, K.; Gustafsdottir, S. M.; Ostman, A.; Landegren, U. *Nat. Biotechnol.* **2002**, *20*, 473–477.
(5) Zhu, H.; Snyder, M. *Curr. Opin. Chem. Biol.* **2003**, *7*, 55–63.
(6) Fan, R.; Vermesh, O.; Srivastava, A.; Yen, B. K. H.; Qin, L.; Ahmad, H.; Kwong, G. A.; Liu, C.; Gould, J.; Hood, L.; Heath, J. R. *Nat. Biotechnol.* **2008**, *26*, 1373–1378.
(7) Vignali, D. A. A. *J. Immunol. Methods* **2000**, *243*, 243–255.
(8) Stoeva, S. I.; Lee, J.; Smith, J. E.; Rosen, S. T.; Mirkin, C. A. *J. Am. Chem. Soc.* **2006**, *128*, 8378–8379.
(9) Qavi, A.; Washburn, A.; Byeon, J.; Bailey, R. *Anal. Bioanal. Chem.* **2009**, *394*, 121–135.
(10) Rich, R. L.; Myszka, D. G. *J. Mol. Recognit.* **2008**, *21*, 355–400.
(11) Teichroeb, J.; Forrest, J.; Jones, L.; Chan, J.; Dalton, K. *J. Colloid Interface Sci.* **2008**, *325*, 157–164.
(12) Ligler, F. S. *Anal. Chem.* **2009**, *81*, 519–526.
(13) Diamandis, E. P. *Mol. Cell. Proteomics* **2004**, *3*, 367–378.
(14) Vaisocherová, H.; Faca, V. M.; Taylor, A. D.; Hanash, S.; Jiang, S. *Biosens. Bioelectron.* **2009**, *24*, 2143–2148.
(15) Armani, A. M.; Kulkarni, R. P.; Fraser, S. E.; Flagan, R. C.; Vahala, K. J. *Science* **2007**, *317*, 783–787.
(16) Zheng, G.; Patolsky, F.; Cui, Y.; Wang, W. U.; Lieber, C. M. *Nat. Biotechnol.* **2005**, *23*, 1294–1301.
(17) Wassaf, D.; Kuang, G.; Kopacz, K.; Wu, Q.; Nguyen, Q.; Toews, M.; Cosic, J.; Jacques, J.; Wiltshire, S.; Lambert, J.; Pazmany, C. C.; Hogan, S.; Ladner, R. C.; Nixon, A. E.; Sexton, D. J. *Anal. Biochem.* **2006**, *351*, 241–253.
(18) Campbell, C. T.; Kim, G. *Biomaterials* **2007**, *28*, 2380–2392.

10.1021/ac9027356
Published on Web 02/11/2010

based SPR is currently commercialized[19] as a platform for screening drug candidates.

Microcantilevers[20−23] are highly sensitive to samples in either purified or simulated media (for example, containing BSA or fibrinogen[24]). They can be scaled to array formats,[25] but detection in undiluted serum has only been demonstrated with the "dip and dry" method[26] or following mass-label amplification.[27] Suspended microchannel resonators (SMRs)[28] are vacuum-packaged silicon microcantilevers with embedded microchannels of picoliter-scale volume (see Figure 1) whose resonant frequency quantifies the mass of the microcantilever. Adsorption of biomolecules to microchannel surfaces displaces an equivalent volume of running solution. The increased density of the biomolecules relative to the displaced solution (proteins are typically 1.35 g/mL)[29] results in a net addition of mass, equivalent to the buoyant mass of the bound biomolecules. This changes the microcantilever resonant frequency in proportion to the amount of bound biomolecules. SMRs are batch-fabricated in a commercial MEMS foundry at approximately 200 devices per 6 in. silicon wafer. Suitable scale-up could make the SMR a platform for routine, inexpensive monitoring of cancer biomarkers with extremely low sample volume and preparation requirements.

We have previously demonstrated[28] the detection of immuno-based protein binding within the SMR; however, the method reported therein was insufficiently specific for sensing in a complex media. Herein, we report an improved label-free surface binding assay for the SMR which enables picomolar detection of a protein target in serum. These improvements were made possible by using a superlow fouling surface based on zwitterionic polymers and a reference microcantilever. Similar polymers have been used in SPR systems to improve specificity of biomolecular detection in undiluted human serum and plasma.[30,31] In this report, we demonstrate that these surfaces in SMRs can be used to enable detection of activated leukocyte cell adhesion molecule (ALCAM) in undiluted serum with a limit of detection of 10 ng/mL. ALCAM is a 105 kDa glycoprotein identified as a potential biomarker for various carcinomas; it is typically found in blood serum at concentrations of ≈84 ng/mL, with levels over 100 ng/mL potentially indicating pancreatic carcinoma.[32]

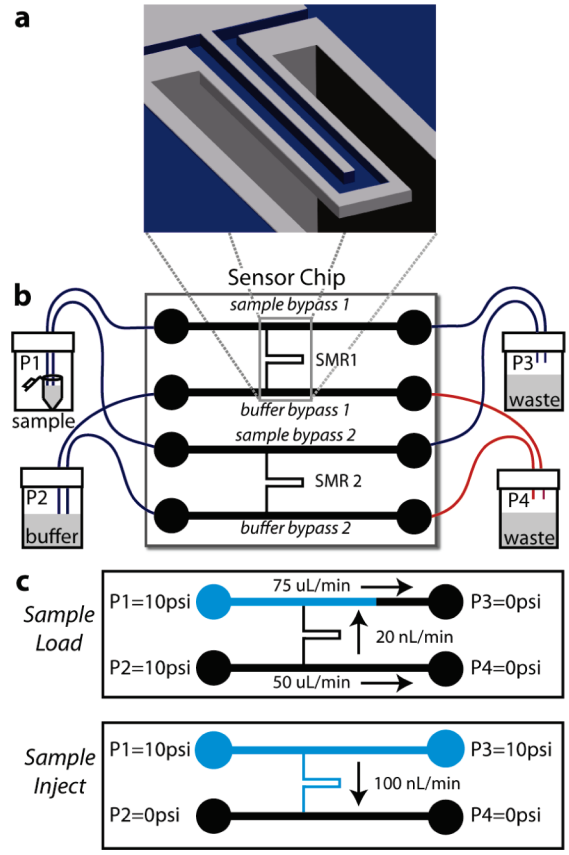

Figure 1. Suspended microchannel resonator (SMR) system schematic. (a) Cut-away view of SMR microcantilever. The U-shaped sensor channel has a 3 × 8 μm^2 cross section and is embedded in a resonating silicon beam extending 200 μm into a vacuum-packaged cavity. (b) Sensor chip with two SMRs addressable by bypass channels connected by Teflon tubing to pressure-controlled vials off-chip; one SMR is used as a control (reference) sensor: blue tubing, i.d. 225 μm; red tubing, i.d. 150 μm. (c) Fluid delivery schemes: "Sample Load" fills sample bypass channels with sample (blue) while the microcantilevers and buffer bypasses are flushed with running buffer (black); "Sample Inject" delivers a sharp concentration sample to the microcantilevers. Figures are not to scale.

MATERIALS AND METHODS

Suspended Microchannel Resonator. The design and structure of SMRs has been described previously.[28] Briefly, each SMR chip contains two vacuum-packaged microcantilevers of resonant frequency of ≈200 kHz with embedded U-shaped microchannels of dimensions 3 μm × 8 μm × 200 μm (height × width × length). Each microcantilever is connected on either end to much larger bypass channels (0.03 mm × 0.1 mm × 12 mm, height × width × length) to allow fast exchange of samples. For small, evenly distributed changes in microcantilever mass, changes in resonant frequency can be described by eq 1:

$$\frac{\Delta f}{f} \approx -\frac{1}{2}\frac{\Delta m}{m} \qquad (1)$$

(19) Säfsten, P.; Klakamp, S. L.; Drake, A. W.; Karlsson, R.; Myszka, D. G. *Anal. Biochem.* **2006**, *353*, 181–190.
(20) Gupta, A.; Akin, D.; Bashir, R. *Appl. Phys. Lett.* **2004**, *84*, 1976–1978.
(21) Li, M.; Tang, H. X.; Roukes, M. L. *Nat. Nano* **2007**, *2*, 114–120.
(22) Lang, H. P.; Berger, R.; Andreoli, C.; Brugger, J.; Despont, M.; Vettiger, P.; Gerber, C.; Gimzewski, J. K.; Ramseyer, J. P.; Meyer, E.; Guntherodt, H. *Appl. Phys. Lett.* **1998**, *72*, 383–385.
(23) Chen, G. Y.; Thundat, T.; Wachter, E. A.; Warmack, R. J. *J. Appl. Phys.* **1995**, *77*, 3618–3622.
(24) Wu, G.; Datar, R. H.; Hansen, K. M.; Thundat, T.; Cote, R. J.; Majumdar, A. *Nat. Biotechnol.* **2001**, *19*, 856–860.
(25) Yue, M.; Stachowiak, J. C.; Lin, H.; Datar, R.; Cote, R.; Majumdar, A. *Nano Lett.* **2008**, *8*, 520–524.
(26) Hwang, K. S.; Lee, S.; Eom, K.; Lee, J. H.; Lee, Y.; Park, J. H.; Yoon, D. S.; Kim, T. S. *Biosens. Bioelectron.* **2007**, *23*, 459–465.
(27) Varshney, M.; Waggoner, P. S.; Tan, C. P.; Aubin, K.; Montagna, R. A.; Craighead, H. G. *Anal. Chem.* **2008**, *80*, 2141–2148.
(28) Burg, T. P.; Godin, M.; Knudsen, S. M.; Shen, W.; Carlson, G.; Foster, J. S.; Babcock, K.; Manalis, S. R. *Nature* **2007**, *446*, 1066–1069.
(29) Fischer, H.; Polikarpov, I.; Craievich, A. F. *Protein Sci.* **2004**, *13*, 2825–2828.
(30) Vaisocherová, H.; Yang, W.; Zhang, Z.; Cao, Z.; Cheng, G.; Piliarik, M.; Homola, J.; Jiang, S. *Anal. Chem.* **2008**, *80*, 7894–7901.
(31) Yang, W.; Xue, H.; Li, W.; Zhang, J.; Jiang, S. *Langmuir* **2009**, *25*, 11911–11916.
(32) Faca, V. M.; Song, K. S.; Wang, H.; Zhang, Q.; Krasnoselsky, A. L.; Newcomb, L. F.; Plentz, R. R.; Gurumurthy, S.; Redston, M. S.; Pitteri, S. J.; Pereira-Faca, S. R.; Ireton, R. C.; Katayama, H.; Glukhova, V.; Phanstiel, D.; Brenner, D. E.; Anderson, M. A.; Misek, D.; Scholler, N.; Urban, N. D.; Barnett, M. J.; Edelstein, C.; Goodman, G. E.; Thornquist, M. D.; McIntosh, M. W.; DePinho, R. A.; Bardeesy, N.; Hanash, S. M. *PLoS Med.* **2008**, *5*, e123.

where f is the resonant frequency and m is the microcantilever mass. Changes in mass (Δm) result only from the contents of the fluidic channel, which includes both the bulk fluid and molecules which adsorb to the channel surfaces.

SMRs were calibrated by measuring the resonance frequency of microcantilevers filled with solutions of known density, resulting in a coefficient of volumetric density change per frequency change. This is converted to surface mass density change by multiplying by microcantilever volume over surface area. Assuming biomolecular densities of 1.35 g/mL[29] and running buffer density 1 g/mL, measured buoyant mass is converted to absolute mass by multiplying by the ratio of biomolecular density over buoyant density (1.35 g/mL over 0.35 g/mL). Experiments in this report were performed on three different SMR chips whose six microcantilevers had calibration coefficients of 46 ± 0.4 (mean ± SD) ng/cm^2/Hz.

During an experiment, both microcantilever frequencies were measured continuously and independently, to allow implementation of a differential sensing scheme with appropriately functionalized sensing and control microcantilevers. Data was acquired in LabVIEW from two synchronized frequency counters (Agilent 53181A) at 2 Hz sampling rate and analyzed in MATLAB. A water bath maintained chip temperature at 25 °C.

Fluids were delivered to the device from pressurized vials (Wheaton W224611) connected to the fluidic bypasses on the SMR via 225 μm i.d. PTFE tubing (Upchurch 1689). Computer-controlled valves selected between atmospheric air and regulated N_2 gas at 10 psi for each vial. Tubing of 150 μm i.d. (red in Figure 1) was used to connect the buffer bypass to waste vials; thus when P1 = P2 and P3 = P4 (*sample loading*) fluid enters the microcantilever from the buffer side and prevents sample solution from entering the microcantilever until the pressures are switched for *sample injection*. To ensure surface reactions were not transport limited, flow velocity in the SMR during sample delivery was large enough to replenish analyte concentration faster than depletion due to binding.[33] Using conservative assumptions for ALCAM diffusivity ($D = 10^{-5}$ cm^2/s) and antibody−target rate constant ($k_{ON} = 1.2 \times 10^6$ cm^3/s/mol), the Damköhler number representing the ratio of maximal binding rates over transport flux was calculated to be $<10^{-2}$.

Synthesis of $DOPA_2$−$pCBMA_2$. (3,4-Dihydroxy-L-phenylalanine)$_2$−(poly(carboxybetaine methacrylate)$_2$) ($DOPA_2$−$pCBMA_2$) was prepared as previously described[34] using atom transfer radical polymerization (ATRP). Briefly, after synthesizing both the initiator, *N*,*N*′-(2-hydroxypropane-1,3-diyl)bis(3-(3,4-bis(*tert*-butyldimethylsilyloxy)phenyl)-2-(2-bromo-2-methylpropanamido)propanamide), and the CBMA monomer, the ATRP reaction was carried out overnight. The subsequent polymer conjugate was purified by dialysis and dried as a white powder. The *tert*-butyldimethylsilyloxy protecting groups were removed using 1 M tetrabutylammonium fluoride in tetrahydrofuran (THF), washed with fresh THF, and then dried under reduced pressure. The remaining white powder was aliquoted and stored at −20 °C until used.

Surface Cleaning and Functionalization. Because of the inert nature of the tubing and the glass and silicon chips, harsh cleaning solutions such as sulfuric acid may be injected enabling device cleaning and reuse. Devices were cleaned as follows: after a 30 min PBS rinse, freshly prepared piranha solution (3:1 mix of H_2SO_4 and H_2O_2) was injected from sample and buffer vials, while the chip was heated to 45 °C by an embedded thermoelectric module. After 30 min, channels were rinsed with deionized water (dH_2O) until all traces of piranha were removed, as the temperature returned to 25 °C. Fresh dH_2O was then injected for 60 min, followed by 30 min of ethanol, followed by 20 min of N_2 gas. Devices were then typically stored dry overnight. Prior to use, fresh dH_2O was injected for 60 min and flow rates were checked visually (by counting the rate of drop formation in waste vial tubes) to ensure sensor and control SMRs had similar flow rates. Cleaned devices typically returned to within 1 Hz of pre-experiment frequencies.

For poly(ethylene glycol) (PEG) fouling tests, poly(L-lysine)−PEG (SuSoS AG, SZ25-46) was reconstituted in PBS at 1 mg/mL and injected for 10 min, resulting in an adsorbed coating as described previously with a similar, biotinylated reagent.[28] For all other experiments, $DOPA_2$−$pCBMA_2$ was reconstituted in dH_2O−HCl (pH 3.0) to a concentration of 2.5 mg/mL and sonicated for 25 min. THF was added to cloud point (≈75% additional volume), and the mixture was injected for 20 min, followed by 10 min of dH_2O injection to quantify adsorption (see Figure 2). For antibody functionalization, carboxylate groups of the $DOPA_2$−$pCBMA_2$ surface were activated by injection of a freshly prepared solution of *N*-hydroxysuccinimide (NHS) (0.05 M) and *N*-ethyl-*N*′-(3-diethylaminopropyl) carbodiimide hydrochloride (EDC) (0.2 M) in dH_2O for 7 min. NHS/EDC was injected through the buffer bypass so as to activate the microcantilever but not the sample bypass surfaces. The dual-bypass design enables this targeted functionalization scheme and prevents target depletion along nonsensing surfaces. Sodium acetate buffer (SA; 10 mM, pH 5.0) was briefly injected to obtain a stable baseline. A solution of antibodies at 50 μg/mL in 1% PBS in dH_2O (pH 10.0) was injected for 14 min. The functionalized surface was washed for 10 min with 10 mM phosphate buffer containing 0.75 M NaCl, pH 8.2, to remove all noncovalently bound ligands. During the protein immobilization, the residual activated groups of $DOPA_2$−$pCBMA_2$ were deactivated. To quantify the amount of immobilized antibodies, SA buffer was injected again for 5 min. A minimum antibody coverage of 90 ng/cm^2 was chosen, and the antibody functionalization procedure (beginning with the NHS/EDC injection) was repeated for experiments whose initial coverage fell below this value. The functionalized surface was then rinsed with PBS for 10 min. Devices filled with stationary PBS were stored for up to 60 min before being used for the experiments shown herein.

Sensing antibodies were mouse anti-ALCAM monoclonal IgGs (R&D Systems, MAB6561). Control antibodies were whole goat IgGs (Abcam, AB37373). Sensing and control microcantilevers were alternated to ensure they would be equivalent.

Measurement of Nonspecific Protein Adsorption and Protein Binding. To test nonspecific protein adsorption, aliquots of fetal bovine serum stored at −20 °C (Sigma-Aldrich, F2442)

(33) Squires, T. M.; Messinger, R. J.; Manalis, S. R. *Nat. Biotechnol.* **2008**, *26*, 417–426.
(34) Zhang, Z.; Zhang, M.; Chen, S.; Horbett, T. A.; Ratner, B. D.; Jiang, S. *Biomaterials* **2008**, *29*, 4285–4291.

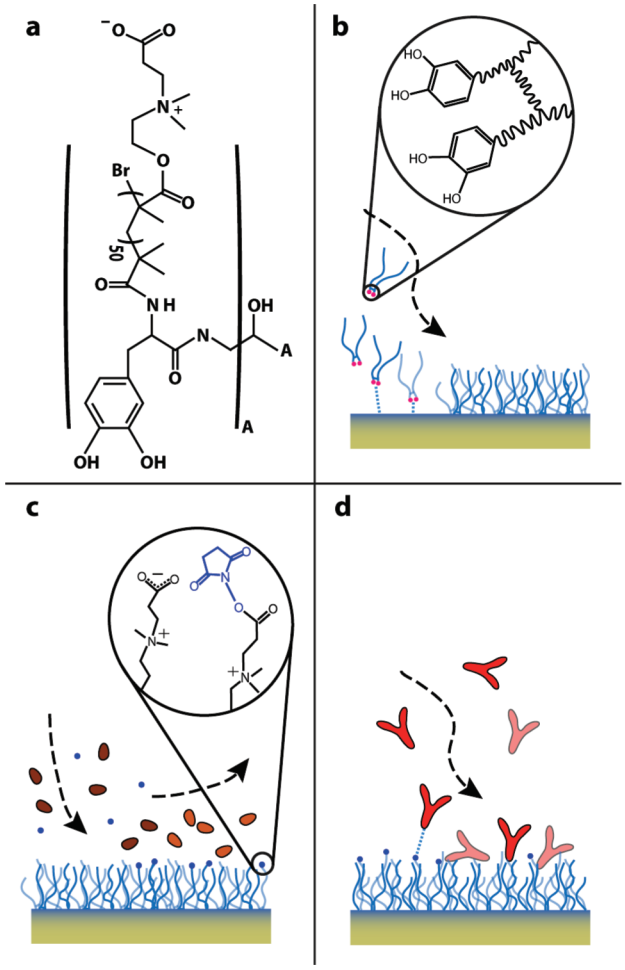

Figure 2. $DOPA_2$−$pCBMA_2$ adsorption and antibody functionalization schematic. (a) The structure of the $DOPA_2$−$pCBMA_2$ polymer is shown; "A" represents the structure inside the large parentheses, two of which are connected by an R−COH−R bridge. The polymer adsorbs directly onto the thin SiO_2 layer of the Si microcantilever surfaces (b), immobilizing a monolayer of 275−360 ng/cm^2. (c) Terminal carboxylic acids are transformed to reactive NHS esters by injection of a mixture of NHS and EDC. (d) NHS esters react with primary amines on IgG antibodies to covalently bind them to the surface.

were thawed, centrifuge-filtered (Millipore, UFC30LG25), and injected for 5 min in the sensing microcantilever functionalized with anti-ALCAM IgG. PBS was injected in the identically functionalized control microcantilever. No blocking step was performed.

For protein binding experiments, human recombinant ALCAM/Fc chimera (R&D Systems, 656-AL-100) was reconstituted in PBS with 1 mg/mL BSA and 0.01% Tween-20, then spiked into serum to a final concentration range of 10−1000 ng/mL. Sample solutions were injected for 10 min followed by PBS rinsing. Prior to sample injections, a blocking solution of 1 mg/mL BSA in PBS was injected for 5 min, followed by a 10 min injection of blank (pure) serum.

RESULTS AND DISCUSSION

$DOPA_2$−$pCBMA_2$ Functionalization. We have previously demonstrated[28] PEG-based SMR surface coatings for biomolecular detection, a technique useful for quantifying purified targets in solution. In nonpurified solutions such as serum, the variability of nonspecific binding severely limited biomolecular resolution. Vaisocherová et al. have previously demonstrated the ability of zwitterionic polymers containing the carboxybetaine moiety to significantly reduce nonspecific adsorption from 100% human plasma, improving on traditional PEG surfaces.[30] Briefly, hydration plays a key role in the prevention of nonspecific protein binding. Zwitterions effectively shield a surface from biomolecular binding by forming a strong hydration layer via electrostatic interactions, compared to the weaker binding of water to PEG, which is based on hydrogen bonding.[35] Furthermore, such surface chemistries were shown to obtain the abundant functional groups necessary for efficient immobilization of protein probes such as antibodies. However, the formation of these carboxybetaine polymer films on the sensing surface required the use of organic solvents and copper-based catalytic systems.

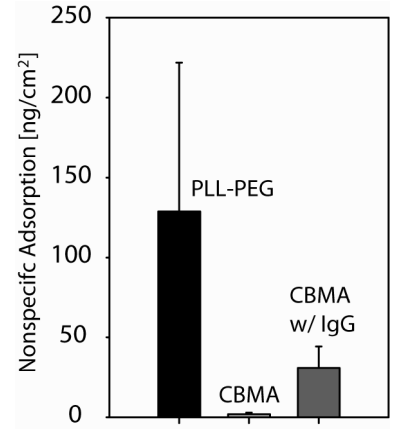

Figure 3. Total nonspecific adsorption after serum injection over PLL−PEG and $DOPA_2$−$pCBMA_2$ surface coatings with and without antibody (IgG) functionalization; n = 3, error bar is 1 SD. Serum incubation time was 5 min, followed by surface washing with PBS for 10 min. The adsorbed layer density was assumed to be 1.35 mg/mL.

The SMR's SiO_2 sensor surface is packaged in a chip and can only be accessed via bypass channels, which limits available reaction conditions and necessitates a different strategy for utilizing carboxybetaine groups. To this end, polymer conjugates based on the adhesive DOPA and pCBMA were created. After first testing these conjugates using an SPR biosensor,[36] the appropriate environment necessary for adsorption onto SMRs was determined. Addition of THF was found to greatly promote $DOPA_2$−$pCBMA_2$ adsorption, which we suspect is due to a decrease in formation of micelles from the amphipathic polymer as the mixture polarity decreased. Optimized conditions led to monolayer surface coverage of 275−360 ng/cm^2, which enabled the direct detection of ALCAM from serum by decreasing the background noise due to nonspecific protein binding compared to our previous PLL−PEG surface functionalization scheme (see Figure 3). Although a detailed mechanism of adsorption on SiO_2 surfaces is not known, Dalsin et al.

(35) Chen, S.; Zheng, J.; Li, L.; Jiang, S. *J. Am. Chem. Soc.* **2005**, *127*, 14473–14478.
(36) Gao, C.; Li, G.; Xue, H.; Yang, W.; Zhang, F.; Jiang, S. *Biomaterials* **2010**, *31*, 1486−1492.

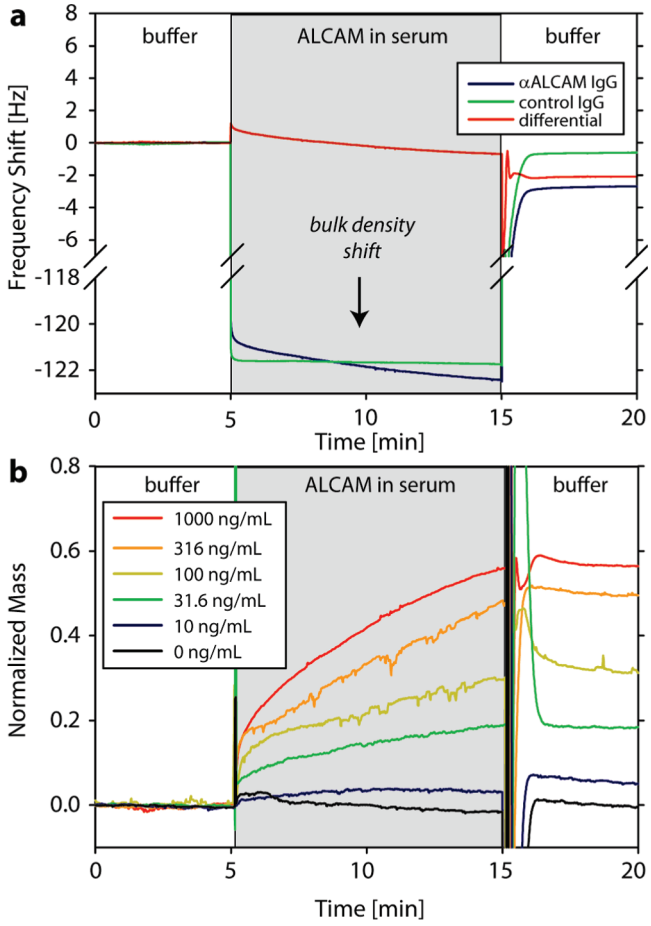

Figure 4. Sensor response to ALCAM-spiked serum on $DOPA_2$–$pCBMA_2$ surfaces functionalized with anti-ALCAM IgG (sensing) and whole goat IgG (control). (a) The mass of specifically bound ALCAM can be quantified by the change in the differential frequency before and after injection of 1000 ng/mL ALCAM. Serum is denser than the PBS running buffer by 1.25%, which results in a −121 Hz bulk density shift during sample injection for both microcantilevers. (b) Dose–response traces for ALCAM injections on de novo functionalized SMR surfaces. The transition from sample to buffer at $t = 15$ min momentarily exhibits large fluctuations due to nonsynchronous rinsing of sensor and control SMRs.

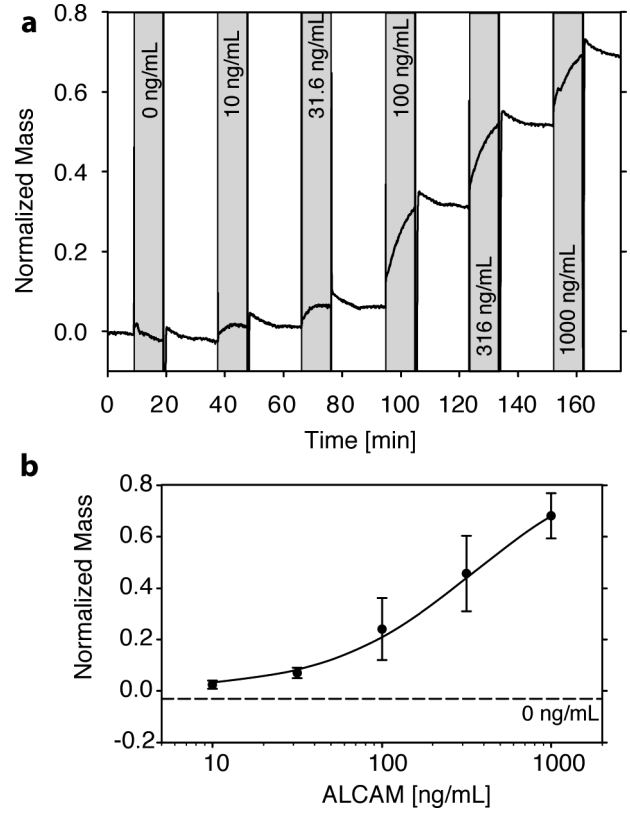

Figure 5. Serial injections of increasing ALCAM concentrations allow construction of a dose–response curve with the same SMR surface. (a) Samples were injected for 10 min each (shaded bars) with an 18 min PBS rinse between samples. (b) Cumulative binding signals ($n = 3$), error bars ±1 SD. The mean response to pure serum (negative control) is plotted as a dashed line (SD = 0.02). The response for each concentration is calculated relative to the initial baseline after the 18 min PBS rinse. The solid line is a variance weighed fit to the Langmuir equation.

previously demonstrated DOPA-terminated polymers to be highly adhesive to TiO_2 surfaces.[37]

Antibody Functionalization and ALCAM Detection. Figure 4 summarizes the dose–response behavior of de novo functionalized $DOPA_2$–$pCBMA_2$ surfaces to varying concentrations of ALCAM in serum. Serum is denser than the PBS buffer by 1.25%, which results in a −121 Hz bulk density shift during the injection (Figure 4a). This shift is not consistent for both microcantilevers due to microcantilever calibrations differing by ≈1% and serum's inhomogeneous density. This leads the differential response during sample injection to be offset by approximately 1 Hz. In Figure 4b, these offsets have been removed for clarity by a MATLAB script that aligns the end of the binding trace during injection with the equilibrium value at the end of the buffer rinse.

Because the IgG antibody functionalization is performed in situ, surface loading of anti-ALCAM IgG can be quantified for each experiment. The IgG loading was found to vary across the six experiments in Figure 4b (101.2–211.6 ng/cm^2), likely due to the rapid breakdown of activated NHS esters and sensitivity to small changes in pH during the IgG functionalization reaction. ALCAM binding data is thus presented as normalized mass units which are calculated as the change in signal due to ALCAM divided by the anti-ALCAM IgG coverage of that experiment. We assumed that the number of active ALCAM binding sites would be linearly correlated with the level of immobilized anti-ALCAM IgG. This interpretation was supported by the consistent ratio of ALCAM signal at saturating concentrations to IgG loading, 0.68 ± 0.09 (mean ± SD). We found no significant correlation between the level of control IgG and ALCAM binding.

To demonstrate repeatability of the dose–response, serial injections of increasing ALCAM concentrations were performed with buffer rinsing but no regeneration of microcantilever surfaces (Figure 5). This approach has the advantages of efficient reagent consumption and shorter experiments.[38] For an ALCAM concentration of 10 ng/mL, with anti-ALCAM IgG loading of 101.2 ng/cm^2, ALCAM loading was 3.9 ng/cm^2. These SMR results were similar in specificity and sensitivity to the response with the

(37) Dalsin, J.; Lin, L.; Tosatti, S.; Vörös, J.; Textor, M.; Messersmith, P. *Langmuir* **2005**, *21*, 640–646.

(38) Abdiche, Y.; Malashock, D.; Pinkerton, A.; Pons, J. *Anal. Biochem.* **2008**, *377*, 209–217.

same anti-ALCAM and ALCAM reagents and a similar carboxybetaine-based surface as measured in a custom-built SPR.[30]

The data presented here illustrates a common disconnect between the sensor technology and the surface chemistry used to develop a bioassay. On one hand the SMR's mass resolution, which is a function of the frequency resolution of the entire system and mass sensitivity of the SMR, is 0.01 ng/cm^2 in a 1 Hz bandwidth.[28] Conservative improvements in microcantilever dimensions would result in an order of magnitude improvement in this sensitivity. On the other hand, for an observed mass signal to be indicative of a target concentration, specificity must be adequate as well. An arbitrary but commonly used standard defines the limit of detection as greater than 3 times the standard deviation of the response to negative controls (here, pure serum) injections, found to be 2.6 ng/cm^2. This more rigorous standard captures both the variability in nonspecific binding from sensor and control surfaces and the effects of sensor drift from the sample injection and rinsing time, which occurs over time scales of 20 min. The 200-fold difference between the SMR limit of detection and the assay limit of detection suggests that further improvements in biomolecular resolution should be pursued in step with improvements in the resolution of the individual sensors.

CONCLUSIONS

We have demonstrated that SMRs functionalized with $DOPA_2$–$pCBMA_2$ surfaces combined with a differential sensing scheme can quantify concentrations of ALCAM, a model cancer biomarker, at physiologically relevant concentrations (10−1000 ng/mL) in undiluted mammalian serum. Micromechanical resonators have hitherto been limited to higher concentrations, multiple assay steps, and/or targets in purified or artificial solutions. Label-free detection in serum was enabled by the use of a zwitterionic, $DOPA_2$–$pCBMA_2$-functionalized surface which significantly reduced nonspecific binding relative to previously reported surfaces. Appropriately functionalized, this surface binds the target molecule, which is detected as a change in resonance frequency proportional to the additional mass of the proteins bound to the sensor surface. SMR signals demonstrate the expected dose−response behavior.

Applicability of this assay to clinical cancer biomarker screening will require further advances in functionalization scheme, device design, and multiplexing capabilities. IgG loading variability in the current work was partly accounted for by normalization but would lead to unacceptable uncertainty in a clinical laboratory setting. Differences in nonspecific binding between the sample and reference microcantilevers may be reduced by adopting more closely integrated sensing and control SMRs, which could be achieved with a single bypass channel feeding multiple microcantilevers. Increasing the number of resonant channels per chip in both serial and parallel configurations will also increase sensitivity and assay throughput.

ACKNOWLEDGMENT

This work was funded by the National Cancer Institute contract R01CA119402 and SAIC-Frederick contract 28XS119. M.G.v.M. was supported by the NIH Biotechnology Training Program. N.D.B. was supported by the Center for Nanotechnology at the University of Washington with funding from an IGERT Fellowship Award NSF #DGE-0504573.

Received for review November 18, 2009. Accepted January 30, 2010.

AC9027356